JOURNAL OF THE ENGINEERING MECHANICS DIVISION

LARGE-DEFLECTION SPATIAL BUCKLING OF THIN-WALLED BEAMS AND FRAMES[a]

By Zdeněk P. Bažant,[1] M. ASCE and Mahjoub El Nimeiri[2]

INTRODUCTION

As is well known, members of most metallic structures, reinforced polymer structures, and some concrete structures must be analyzed, in the simplest approximation, as thin-walled beams whose cross section exhibits significant out-of-plane warping due to torsion (28,38,40). Planar failure modes of such structures are known to be an exception rather than a rule. Yet, nearly all studies of large deflections and post-buckling behavior have so far been confined to planar (or to local) deformation modes and the buckling studies of thin-walled structures have been restricted to the bifurcation problem, to small deflections, and (except for a few special cases) to straight members. An exception are a few studies (10,14,18) in which the post-buckling behavior in lateral buckling of straight thin-wall beams was investigated analytically, solving by the Galerkin method a nonlinear differential equation based on some simplifying assumptions (10). However, the analytical approach would be too complicated in the case of complex structures.

The aim of the present study is to develop a general matrix stiffness analysis of spatial large deflections and of post-buckling behavior of thin-walled straight or curved beams, frames, and arches that are not excessively slender. This development will, of course, also enable analysis of spatial (lateral) buckling in bifurcation problems for arbitrary, not too slender, curved beams and arches, for which no method is presently available. The formulation will be given for

Note.—Discussion open until May 1, 1974. To extend the closing date one month, a written request must be filed with the Editor of Technical Publications, ASCE. This paper is part of the copyrighted Journal of the Engineering Mechanics Division, Proceedings of the American Society of Civil Engineers, Vol. 99, No. EM6, December, 1973. Manuscript was submitted for review for possible publication on December 28, 1972, and was revised on August 8, 1973.

[a]Presented at the October 16-22, 1972, ASCE Annual and National Environmental Engineering Meeting, held at Houston, Tex.

[1]Prof. of Civ. Engrg., Northwestern Univ., Evanston, Ill.

[2]Grad. Student, Dept. of Civ. Engrg., Northwestern Univ., Evanston, Ill.

an arbitrary asymmetric open cross section.

The analysis of thin-walled structural systems was first approached using the method of transfer matrices (40) and the force (flexibility) method (7,11,12, 17,39,40). These methods are, however, much less versatile than the displacement (stiffness) method. The stiffness matrix of a thin-walled beam element seems to have been first presented in 1967 by Krahula (22), for the case without initial stress, and by Renton (34), who included the effect of initial axial force on bending stiffness. With inclusion of initial bending moments and initial axial force, it was derived by Krajcinovic (23), Barsoum and Gallagher (6), Powell and Klingner (31), Mei (26), and Rajasekaran (33). The stiffness matrix which includes initial bimoment will be derived herein. Apparently, it has not yet been given in the literature, probably because this matrix is needed only for the large deflection analysis, and also because no bifurcation-type buckling can be induced by a bimoment. Argyris and Radaj (2) deduced the stiffness matrix with account of secondary shear strains and elastic stiffeners, but without initial stresses. The mass matrix was given by Krajcinovic (23) and Mei (26).

While most authors assumed cubic variation of all displacement parameters along the member, Krajcinovic (23) argued that exact static influence functions must be used instead, claiming that cubic polynomials lead to large errors whenever the ratio of Saint-Venant torsional rigidity to warping torsional rigidity is not negligible. This claim, however, has been disproved by Mei (27), as well as by the numerical results of the writers.

The relation between the warping parameters and bimoments at the coincident ends of two elements meeting at an angle apparently has not yet been determined and will be derived herein. It is needed for the analysis of curved members approximated by a series of straight elements, and also for the incremental loading approach to large deflections of beams which are straight prior to loading. Because it will be convenient to refer some element displacements and forces to the shear center and others to the centroid, a transformation matrix between these two frames of reference will have to be deduced.

POTENTIAL ENERGY OF THIN-WALLED BEAMS UNDER INITIAL STRESS

It is well known that sufficiently long shells can be analyzed as thin-walled bars. In the case of open cross section, which will solely be considered in the sequel, the analysis is reduced to a one-dimensional beam problem with the help of three simplifying assumptions:-(1) The cross section is assumed to be perfectly rigid in its plane while free to warp out of its plane; (2) the shear strains in the middle surface of the shell are neglected (Wagner's assumption); and (3) the transverse normal stresses and all bending moments in the shell wall are neglected. Furthermore, the material is assumed to be linearly elastic and the strains small, although the deflections and rotations may be large.

The first two assumptions yield for the longitudinal displacement, u_z, at any point of the cross section (38,40)

$$u_z = \zeta(z) - \bar{\xi}'(z)\, x(s) - \bar{\eta}'(z)\, y(s) - \theta'(z)\, \bar{\omega}(s) \quad \ldots\ldots\ldots\ldots (1)$$

in which z = the length coordinate of the beam (Fig. 1); primes are used to denote derivatives with respect to z, e.g., $\theta' = d\theta/dz$; x, y = principal centroidal

axes of the cross section forming a right-handed system together with z (Fig. 1) [in contrast with the more common use of a left-handed system (40)]; ζ = z-displacement at the centroid; $\bar{\xi}$, $\bar{\eta}$ = x and y displacements at the shear center C (40); θ = rotation of cross section about axis z; and $\bar{\omega}$ = principal sectorial area coordinate for a pole in shear center C (38,40), defined as $\bar{\omega} = \int_0^s \rho(s')ds'$ where ρ = distance of wall tangent from C, and s = length coordinate of cross section measured from the sectorial null point (40); $\rho\, ds'$ is positive when ds' turns radius ρ counterclockwise (as θ in Fig. 1), which is counter the usual sign convention (40). All quantities referred to the shear center rather than the centroid are labeled by bars, and unlabeled quantities refer to the centroid. Quantities of both types will be mixed because this will lead to simpler final expressions. (Note that Eq. 1 is equivalent to the usual expression $\zeta - \xi' x - \eta' y - \theta' \omega$ in which all quantities refer to the centroid.) Coordinate $\bar{\omega}$ differs only by a constant from the warping function, ω_s, of Timoshenko and Gere (38). Their use of bars is different. The present notation, which is consistent with refs. 7, 8, 21, 23, 40, is more concise in case of asymmetric cross sections.

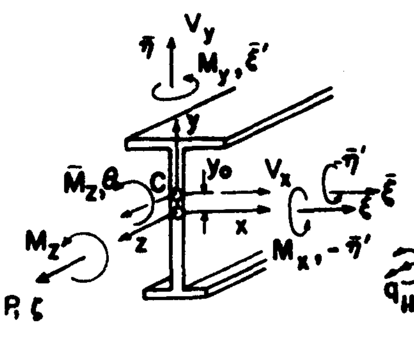

FIG. 1.—Coordinate Axes, Displacements, and Internal Forces in Thin-Wall Beam

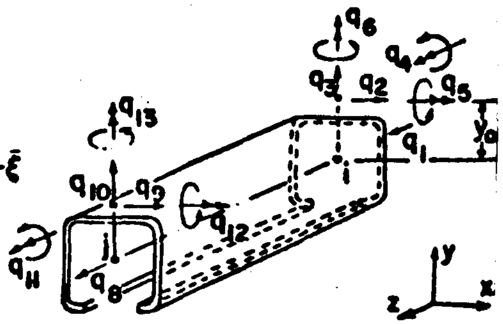

FIG. 2.—Generalized Displacements of Thin-Walled Beam Element (θ' Not Shown)

Mathematically, Eq. 1 can be regarded as an assumption for the first four terms of Kantorovich direct variational method, with 1, $x(s)$, $y(s)$, $\bar{\omega}(s)$ as the chosen orthogonal functions (8).

Consider now that the beam is initially in equilibrium at normal stress σ_z^0 due to initial axial force P^0 (positive for tension), initial bending moments M_x^0, M_y^0 about principal centroidal axes x and y (of sign shown in Fig. 1), and initial bimoment $\bar{B}^0$ referred to the shear center. Thus (38,40)

$$\sigma_z^0 = \frac{P^0}{A} + \frac{M_x^0}{I_x} y - \frac{M_y^0}{I_y} x - \frac{\bar{B}^0}{I_{\bar{\omega}}} \bar{\omega} \quad \ldots \quad (2)$$

in which $\bar{B}^0 = -\int_A \sigma_z^0 \bar{\omega}\, dA$; A = area of cross section; $I_x = \int_A y^2 dA$ and $I_y = \int_A x^2 dA$ are the moments of inertia about centroidal axes x and y; and $I_{\bar{\omega}} = \int_A \bar{\omega}^2 dA$ = principal sectorial moment of inertia. [Quantity $I_{\bar{\omega}}$ is identical with the warping constant, C_w, of Timoshenko and Gere (38).]

Subsequently, small increments of loads are superimposed upon the loads

in the initial state, producing displacements $\bar{\xi}$, $\bar{\eta}$, ζ, θ, now considered as displacement increments with regard to the initial equilibrium state. The associated incremental potential energy is

$$\Delta U = \Delta U_1 + \Delta U_0 - \Delta W \quad \ldots \quad (3)$$

in which ΔW = work of load increments on $\xi, \ldots, \theta$, and

$$\Delta U_1 = \int_z \int_A \frac{1}{2} E e_z^2\, dA dz + \int_z \frac{1}{2} G I_s \theta'^2 dz \quad \ldots \quad (4)$$

$$\Delta U_0 = \int_z \int_A \sigma_z^0 \epsilon_z\, dA dz + \int_z M_s^0 \theta'\, dz \quad \ldots \quad (5)$$

in which ΔU_1 = incremental strain energy; ΔU_0 = energy due to initial stresses; GI_s = Saint-Venant's rigidity in simple torsion (38,40); M_s^0 = initial Saint-Venant's torque; e_z = small (linearized) strain; and ϵ_z = finite strain, i.e.

$$e_z = \frac{\partial u_z}{\partial z}; \quad \epsilon_z = e_z + \frac{1}{2}\left(\frac{\partial u_x}{\partial z}\right)^2 + \frac{1}{2}\left(\frac{\partial u_y}{\partial z}\right)^2 \quad \ldots \quad (6)$$

in which u_x, u_y = displacements of a general point of cross section in x- and y-directions. According to the assumption of rigid cross sections

$$u_x = \bar{\xi}(z) - (y - y_0)\theta(z); \quad u_y = \bar{\eta}(z) + (x - x_0)\theta(z) \quad \ldots \quad (7)$$

in which x_0, y_0 = coordinates of shear center (40).

Eq. 4 involves small strain e_z because only infinitesimally small incremental deformation is considered. Nevertheless, in Eq. 5, the finite strain expression must be used, because, in view of σ_z^0 being finite (large), $\sigma_z^0 e_z$ would be accurate only up to small quantities of the first order in the displacement gradients while Ee_z^2 is a small quantity of second order (9). But component $1/2(\partial u_z/\partial z)^2$ of ϵ_z has been deleted from ϵ_z since for small incremental strains it is negligible with regard to e_z. The work of initial Saint-Venant torque M_s^0 in Eq. 5 includes no second-order small term.

Substitution of Eq. 7 into Eq. 6, and Eqs. 2 and 6 into Eqs. 4 and 5, leads to the following expressions

$$\Delta U_1 = \int_z \frac{1}{2}\left[E(A\zeta'^2 + I_y \bar{\xi}''^2 + I_x \bar{\eta}''^2 + I_{\bar{\omega}}\theta''^2) + GI_s\theta'^2\right] dz \quad \ldots \quad (8)$$

$$\Delta U_0 = P^0 \int_z \left(\zeta' + \frac{1}{2}\bar{\xi}'^2 + \frac{1}{2}\bar{\eta}'^2 + \frac{1}{2} r^2 \theta'^2 + y_0 \bar{\xi}'\theta' - x_0 \bar{\eta}'\theta'\right) dz$$
$$- M_x^0 \int_z (\bar{\eta}'' - \beta_y \theta'^2 + \bar{\xi}'\theta')\, dz + M_y^0 \int_z (\bar{\xi}'' - \beta_x \theta'^2 - \bar{\eta}'\theta')\, dz$$
$$+ \bar{B}^0 \int_z \left(\theta'' - \frac{1}{2}\bar{W}\theta'^2\right) dz \quad \ldots \quad (9)$$

in which $r^2 = x_0^2 + y_0^2 + \dfrac{I_x + I_y}{A}$; $\bar{W} = \int_A \bar{\omega}(x^2 + y^2)\, dA \Big/ I_{\bar{\omega}}$

$$\beta_y = \frac{1}{2I_x}\int_A y(x^2+y^2)\,dA - y_0; \quad \beta_x = \frac{1}{2I_y}\int_A x(x^2+y^2)\,dA - x_0 \qquad (10)$$

Note that for a doubly symmetric cross section $W = 0$, and so $\bar{B}^0$ does not contribute to ΔU_0.

Because the preceding equations for incremental potential energy in the presence of initial stress are not available in the literature, it has been checked that the Euler differential equations obtained from Eqs. 8 and 9 by variational calculus are the same as those derived by Vlasov from considerations of adjacent equilibrium configurations (Eqs. 1.10 of Chap. V or 1.28 of Chap. VI, and Eq. 15.3 of Chap. V, in Ref. 40). One can also verify that the natural boundary conditions associated with Eqs. 8 and 9 are the same as those resulting from Eq. 16. Note that Eqs. 9 and 10 apply for an arbitrary nonsymmetric cross section.

In the practically prevalent case of a cross section symmetric with respect to axis y, the foregoing equations simplify since $x_0 = \beta_x = 0$; $\bar{\omega} = \omega + y_0 x$; $y_0 = -I_{\omega x}/I_y$, in which $I_{\omega x} = \int_A \omega\, x\, dA$, and ω = sectorial area coordinate referred to the centroid; $\bar{B} = B + M_y y_0$, in which $B = -\int_A \sigma_z\, \omega\, dA = EI_\omega \theta''$ = bimoment referred to the centroid; and $\bar{\xi} = \xi - \theta y_0$, $\bar{\eta} = \eta$. In the case of double symmetry, $y_0 = \beta_y = 0$, $\bar{\omega} = \omega$, $\bar{B} = B$, and $\bar{\xi} = \xi$.

Stiffness of Thin-Walled Beam Elements Under Initial Stress

The stiffness matrix will have by far the simplest form if some quantities are referred to the shear center and others to the centroid, as has been already introduced (in contrast with the current practice in finite elements for beams). Referring to Eq. 1, it is clear that the displacements in the cross section are fully characterized by seven generalized displacements ζ, $\bar{\xi}$, $\bar{\eta}$, θ, $-\bar{\eta}'$, $\bar{\xi}'$, θ', of which the first six describe the rigid body motions of cross section and the last one is the warping parameter. Thus, the column matrix, $\mathbf{q}$, of generalized displacements of a beam element (Fig. 2) has the components

$$\mathbf{q} = (\zeta_i, \bar{\xi}_i, \bar{\eta}_i, \theta_i, -\bar{\eta}_i', \bar{\xi}_i', \theta_i', \zeta_j, \bar{\xi}_j, \bar{\eta}_j, \theta_j, -\bar{\eta}_j', \bar{\xi}_j', \theta_j')^T \qquad (11)$$

in which subscripts i, j refer to end cross sections i, j and superscript T stands for the transpose of the matrix.

For approximation of the stiffness matrix of the element, ζ, $\bar{\xi}$, $\bar{\eta}$, and θ will be assumed as:

$$\left.\begin{aligned} &\zeta = a_1 + b_1 z; \quad \bar{\xi} = a_2 + b_2 z + c_2 z^2 + d_2 z^3 \\ &\bar{\eta} = a_3 + b_3 z + c_3 z^2 + d_3 z^3; \quad \theta = a_4 + b_4 z + c_4 z^2 + d_4 z^3 \end{aligned}\right\} \qquad (12)$$

in which $a_1, b_1, a_2, \ldots, d_4$ are arbitrary constants. Altogether, there are 14 arbitrary constants, which can thus be expressed in terms of the 14 components of $\mathbf{q}$, giving a relation of the form

$$(\zeta, \bar{\xi}, \bar{\eta}, \theta)^T = \mathbf{N}(z)\mathbf{q} \qquad (13)$$

in which $\mathbf{N}(z) = (4 \times 14)$ matrix whose coefficients are certain cubic polynomials in z (matrix of shape functions). To ensure convergence, the rigid body rotations without straining and the states of constant $\bar{\xi}''$, $\bar{\eta}''$, ζ', θ', θ'' must be available.

It is easy to check that Eqs. 12 satisfy these conditions.

Substituting Eq. 13 into Eqs. 8 and 9, incremental potential energy ΔU (Eq. 3), is obtained as a quadratic form in $\mathbf{q}$. As is well known, the elements of incremental (tangential) stiffness matrix $\mathbf{K} = [K_{ij}]$, (14×14) in size, are then obtained as

$$K_{ij} = \frac{\partial^2 \Delta U}{\partial q_i \partial q_j} \qquad (14)$$

Carrying out the differentiation, the incremental stiffness matrix is obtained as a linear function of the initial internal forces, i.e.

$$\mathbf{K} = \mathbf{K}_0 + P^0\mathbf{K}_1 + M_x^0\mathbf{K}_2 + M_y^0\mathbf{K}_3 + \bar{B}^0\mathbf{K}_4 \qquad (15)$$

in which $\mathbf{K}_0$ depends on the elastic moduli and is called elastic stiffness matrix, while matrices $\mathbf{K}_1$, $\mathbf{K}_2$, $\mathbf{K}_3$, $\mathbf{K}_4$ are independent of the elastic moduli and are called geometric stiffness matrices. All of these matrices are symmetric. The nonzero elements of the upper triangular part of $\mathbf{K}$ are

$$K_{11} = -K_{18} = K_{88} = \frac{EA}{l}; \quad K_{22} = -K_{29} = K_{99} = \frac{12k_y}{l^3} + \frac{6}{5l}P^0;$$

$$K_{24} = -K_{211} = K_{911} = -K_{49} = -\frac{6}{5l}M_x^0 + \frac{6y_o}{5l}P^0; \quad K_{26} = K_{213} =$$

$$-K_{69} = -K_{913} = \frac{6k_y}{l^2} + \frac{P^0}{10}; \quad K_{27} = K_{214} = -K_{914} = -K_{611} = K_{46}$$

$$= K_{413} = -K_{79} = -K_{1113} = -\frac{1}{10}M_x^0 + \frac{y_o P^o}{10}; \quad K_{33} = -K_{310} = K_{1010}$$

$$= \frac{12k_x}{l^3} + \frac{6}{5l}P^0; \quad K_{34} = -K_{311} = -K_{410} = K_{1011} = -\frac{6}{5l}M_y^o;$$

$$K_{35} = K_{312} = -K_{510} = -K_{1012} = -\frac{6k_x}{l^2} - \frac{P^0}{10};$$

$$K_{37} = K_{314} = -K_{1014} = -\frac{1}{10}M_y^o; \quad K_{44} = -K_{411} = K_{1111}$$

$$= \left(12 + \frac{6}{5}\kappa^2\right)\frac{C_1}{l^3} + \frac{6r^2}{5l}P^0 + \frac{12\beta_y}{5l}M_x^o - \frac{6}{5l}\bar{W}\bar{B}^0;$$

$$K_{45} = K_{412} = -K_{1112} = -K_{511} = -K_{710} = \frac{-1}{10}M_y^0;$$

$$K_{47} = K_{414} = -K_{711} = -K_{1114} = \left(6 + \frac{\kappa^2}{10}\right)\frac{C_1}{l^2} + \frac{r^2}{10}P^0$$

$$-\frac{\beta_y}{5}M_x^0 - \frac{\bar{W}}{10}\bar{B}^0; \quad K_{55} = K_{1212} = \frac{4k_x}{l} + \frac{2}{15}lP^0;$$

$$K_{5\,7} = K_{12\,14} = \frac{-2}{15} M_y^o; \quad K_{5\,14} = K_{7\,12} = \frac{l}{30} M_y^0;$$

$$K_{5\,12} = \frac{2k_x}{l} - \frac{l}{30} P^0; \quad K_{6\,6} = K_{13\,13} = \frac{4k_y}{l} + \frac{2l}{15} P^0;$$

$$K_{6\,7} = K_{13\,14} = -\frac{2}{15} M_x^0 + \frac{2}{15} y_o P^o; \quad K_{6\,13} = \frac{2k_y}{l} - \frac{l}{30} P^0;$$

$$K_{6\,14} = K_{7\,13} = \frac{l}{30} M_x^0 - \frac{l}{30} y_o P^o;$$

$$K_{7\,7} = K_{14\,14} = \left(4 + \frac{2\kappa^2}{15}\right)\frac{C_1}{l} + \frac{2}{15} r^2 l P^0 + 4\frac{l\beta_y}{15} M_x^0 - \frac{2l}{15} \bar{W}\bar{B}^0;$$

$$K_{7\,14} = \left(2 - \frac{\kappa^2}{30}\right)\frac{C_1}{l} - \frac{lr^2 P^0}{30} - \frac{l}{15}\beta_y M_x^0 + \frac{\bar{W}l}{30}\bar{B}^0 \quad \ldots\ldots\ldots\ldots (16)$$

in which l = length of element

$$k_x = EI_x; \quad k_y = EI_y; \quad \kappa^2 = l^2\frac{C}{C_1}; \quad C = GI_s; \quad C_1 = EI_{\bar{\omega}}; \quad \bar{W} = \frac{W}{I_{\bar{\omega}}} \qquad (17)$$

Note that $K_{ij} = K_{i-7,j-7}$ or $K_{i-7,j+7}$ for $i > 7$. Also note that Eq. 16 applies for arbitrarily asymmetric cross section. It has been checked that the special case of stiffness matrix for a planar case and a mono-symmetric cross section with $\bar{B}^0 = 0$, and for a simplified account of simple torsion, as presented in Refs. 6 or 31, agrees with Eq. 16. The special case of stiffness matrix without initial stress, presented in Ref. 26, is also in agreement.

The column matrix, $\mathbf{F}$, of associated incremental generalized forces at the ends of the element ensues from the condition that $\mathbf{F}^T\mathbf{q}$ must give the correct value of work for any $\mathbf{q}$. This is true if, and only if

$$\mathbf{F} = (P_i, \bar{V}_{x_i}, \bar{V}_{y_i}, \bar{M}_{z_i}, M_{x_i}, M_{y_i}, \bar{B}_i, P_j, \bar{V}_{x_j}, \bar{V}_{y_j}, \bar{M}_{z_j}, M_{x_j}, M_{y_j}, \bar{B}_j)^T \qquad (18)$$

in which P = incremental axial force (acting in the centroid); $\bar{V}_x, \bar{V}_y$ = incremental shear forces (acting in the shear center); $\bar{M}_z$ = incremental torque about shear center; M_y, M_x = incremental bending moments about centroidal axes x and y (Fig. 2); and $\bar{B} = -\int_A \sigma_z \bar{\omega}\, dA$ = incremental principal bimoment, referred to the shear center.

Curved Beams Approximated by Straight Elements and Beams of Variable Cross Section

The simplest method of analysis of a curved beam is based on approximating the beam by a series of straight elements. For this purpose it is necessary to deduce the transformation matrix, $\mathbf{T}$, which transforms the generalized forces and displacements at the end j of element ij to those at the end j of the adjacent

element jk meeting at an angle at the joint j (Fig. 3) or, alternatively, to global coordinates. All elements of matrix $\mathbf{T}$ can be determined from kinematics, except those which multiply θ' or $\bar{B}$. The latter ones seem to have eluded attention so far. They cannot be ascertained merely by consideration of u_z-distributions at the end j of elements ij and jk (Fig. 3) because these distributions are incompatible for any nonzero angle between the elements. This fact need not be viewed as objectionable because the finite elements approximate, in the first place, the one-dimensional curved beam problem, and not the actual three-dimensional problem which does not involve the simplifying assumptions of thin-walled beam theory.

In view of this fact, it will be imagined that the approximation by straight elements is the limiting case of a beam consisting of straight elements interconnected by means of short curved elements (Fig. 4) whose length L tends to

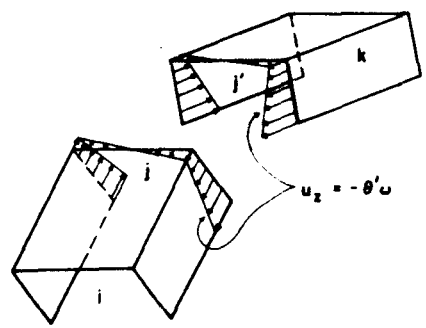

FIG. 3.—Incompatibility of Assumed Warping Displacement Distributions u_z when Two Elements Meet at Angle

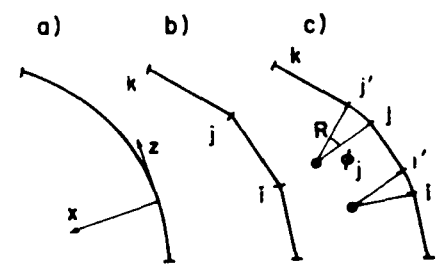

FIG. 4.—Approximation of Curved Beam (a) by Beam Consisting of Straight Elements (b), and Transition from (a) to (b) Through a Beam with Straight and Curved Segments (c)

zero. To this end it is necessary to find the transfer matrix, $\mathbf{T}'$, of the curved element, jj', in Fig. 4, defined by the relation

$$\mathbf{S}_{j'} = \mathbf{T}'\,\mathbf{S}_j \quad \ldots\ldots\ldots\ldots\ldots\ldots\ldots\ldots\ldots\ldots\ldots\ldots (19)$$

in which subscripts j, j' refer to cross sections j, j' (Fig. 4); $\mathbf{S}$ = the state vector for the cross section, which may be defined in the case of circularly curved members (40) as

$$\mathbf{S} = \left(\zeta, \bar{\xi}, \bar{\eta}, \theta, -\bar{\eta}', \bar{\xi}', \theta' + \frac{\eta'}{R}, P, \bar{V}_x, \bar{V}_y, \bar{M}_z, M_x, M_y, \bar{B}\right)^T \quad \ldots (20)$$

For examining the transformation of $\bar{B}$ and θ', the connecting element, jj', will be considered as a circularly curved thin-walled beam of radius R, with the center of curvature on the positive side of axis x and cross section symmetric about axis y. No initial forces and no distributed loads will be considered. Deformations of this beam are known to be governed by the differential equations (Eq. 1.10 of Chap. XII in Ref. 40):

$$\left.\begin{aligned}(L^2+R^2c^2)\eta^{IV}-\kappa^2\eta''+RL^2\theta^{IV}-R(c^2+\kappa^2)\theta''=0\\ L^2\eta^{IV}-(c^2+\kappa^2)\eta''+RL^2\theta^{IV}-R\kappa^2\theta''+\frac{\theta c^2}{R}=0\end{aligned}\right\} \quad \ldots\ldots\ldots (21)$$

in which $c^2 = L^2EI_x/EI_{\bar{\omega}}$; $\kappa^2 = L^2GI_s/EI_{\bar{\omega}}$; and θ = rotation about shear center. The exact transformation matrix, $\mathbf{T}'$, has been derived by integration of these equations and is given in the Appendix. Letting $L \to 0$ and $R \to 0$ while keeping $\phi_j = L/R$ constant (Fig. 4), the limit of $\mathbf{T}'$ is the sought for transformation matrix, $\mathbf{T}$.

In the manner just explained it has been found that

$$\mathbf{T} = \lim_{R\to 0} \mathbf{T}' = \begin{bmatrix} \mathbf{R} & & & \\ & \mathbf{R} & & \\ & & 1 & \\ & & & \mathbf{R} \\ & & & & \mathbf{R} \\ & & & & & 1 \end{bmatrix} \quad \ldots\ldots\ldots (22)$$

in which $\mathbf{R}$ = the (3 × 3) rotation matrix as given in Ref. 32. As is seen, $\mathbf{T}$ has a very simple form, for which $\mathbf{T}^{-1} = \mathbf{T}^T$. The same result can reasonably be expected to hold for a noncircular nonplanar curvature and in presence of initial stress. Aside from the columns and rows pertaining to θ' and $\bar{B}$, the structure of $\mathbf{T}$ can, naturally, be determined from rigid body kinematics.

The unity coefficients in Eq. 22 can also be obtained by simple intuitive reasoning. If the columns relating to θ' and $\bar{B}$ had nonzero elements outside the diagonal, warping θ' would produce a rigid body displacement in the same joint and bimoment $\bar{B}$ would result in an internal force or moment in the same joint, both of which would be unacceptable features. So only the diagonal terms of the columns considered may be nonzero. If the rows relating to θ' and $\bar{B}$ had nonzero elements outside the diagonal, rigid body displacements could not occur without causing a warping in the same joint, and internal forces and moments would cause a bimoment, both of which are again impossible. Thus only the diagonal terms of the considered rows may be nonzero. Consider now that $\theta'_i = a\,\theta'_j$. The same transfer coefficient must apply in the reverse direction, i.e., $\theta'_j = a\,\theta'_i$. This is possible only if $a = 1$. Similar considerations show that the diagonal coefficient for $\bar{B}$ must be also 1.

The foregoing argument, however, does not verify consistency with the differential equations of the problem, which is an important aspect to be checked because the u_z-distributions in the cross sections of the interacting straight elements are incompatible. Alternatively, Eq. 22 could also be derived from the natural boundary conditions of curved beam segment ij (Fig. 4). Note that Eq. 22 has already been implied in Ref. 21 without offering any justification.

The simple form of matrix $\mathbf{T}$ makes the approximation of curved beams by straight elements particularly advantageous.

Beams of variable cross section may be approximately treated using elements of constant cross section which represent the average cross section of the actual

beam within the interval considered. The u_z-displacements from the adjacent elements are then, of course, incompatible. But it is consistent with the ordinary differential equations for beams of variable cross section (7) to consider that θ' and B are continuous between the elements of different cross section, as has been proved in Ref. 7.

Transformation to Global Coordinates and to Centroidal Axes

Rather than transforming $\mathbf{q}$ from local coordinates x, y, z of one element into the local coordinates x, y, z of the adjacent element, it is more convenient in practical computations to transform $\mathbf{q}$ of each element into global coordinates X, Y, Z of the structure. Observing that the transformation matrix for element displacement column vector $\mathbf{q}$ is the same as for state vector $\mathbf{S}$, one obtains

$$\mathbf{q}^* = \mathbf{T}\,\mathbf{q} \quad \ldots\ldots\ldots (23)$$

in which $\mathbf{q}^*$ = column matrix of element displacements transformed to global coordinates; and $\mathbf{T}$ = matrix of form of Eq. 22 with rotation matrix $\mathbf{R}$

$$\mathbf{R} = \begin{bmatrix} a_X & a_Y & a_Z \\ b_X & b_Y & b_Z \\ c_X & c_Y & c_Z \end{bmatrix} \quad \ldots\ldots\ldots (24)$$

in which (a_X, a_Y, a_Z), (b_X, b_Y, b_Z), (c_X, c_Y, c_Z) are the global coordinates of the unit vectors $\mathbf{a}$, $\mathbf{b}$, $\mathbf{c}$ of the axes x, y, z of the element.

The transformation matrix, $\mathbf{T}$, given by Eq. 22 applies, however, only when all components of $\mathbf{q}$ are referred to the same point in the cross section, which is true only for doubly symmetric cross sections. Otherwise, it is necessary to transform first displacement matrix $\mathbf{q}$ into matrix $\mathbf{q}^c$ all of whose components are referred to the cross-sectional centroid. This transformation may be written as

$$\mathbf{q}^c = \mathbf{t}\,\mathbf{q} \quad \ldots\ldots\ldots (25)$$

in which $\mathbf{t}$ = (14 × 14) matrix all of whose diagonal terms = 1 and, taking a monosymmetric cross section as an example, the nonzero off-diagonal terms represent the relations $\xi = \bar{\xi} + y_0$, and $\xi' = \bar{\xi}' + \theta' y_0$. Similarly, force matrix $\mathbf{F}$ is transformed into $\mathbf{F}^c$ and, in conformity with the general rules in matrix structural analysis

$$\mathbf{F} = \mathbf{t}^T\mathbf{F}^c \quad \ldots\ldots\ldots (26)$$

That this is indeed so may be checked by deriving $\mathbf{t}^T$ directly from the fact that the nonzero off-diagonal terms of $\mathbf{t}^T$ must correspond to the relations $\bar{M}_z = M_z + V_x y_0$, $\bar{B} = B + M_y y_0$, in the case of monosymmetry.

Thus, for asymmetric or monosymmetric cross sections, the transformation matrix to global coordinates which also includes tranformation of all components to the cross section centroid is

$$\mathbf{T} = \mathbf{t}\,\mathbf{T}_1\,\mathbf{t}^{-1} \quad \ldots\ldots\ldots (27)$$

in which $\mathbf{T}_1$ = the matrix given by Eq. 22. For example, in the case of a

monosymmetric cross section, T can be obtained by carrying out the matrix multiplications in Eq. 27. This yields

$$\mathbf{T} = \begin{bmatrix} \mathbf{R} & \begin{matrix} -y_0 a_y \\ y_0(a_x - b_y)\; y_0 a_y\; y_0 a_z \\ -y_0 c_y \end{matrix} & \begin{matrix} \\ -y_0^2 a_z \\ \\ \end{matrix} \\ \hline & \begin{matrix} \\ \mathbf{R} \\ \\ \end{matrix} & \begin{matrix} -y_0 a_z \\ -y_0 b_z \\ y_0(1 - c_z) \\ 1 \end{matrix} \\ \hline & & \text{ditto} \end{bmatrix} \tag{28}$$

The stiffness matrix and the column matrix of generalized forces are then transformed to (or from) the global coordinates as

$$\mathbf{K}^* = \mathbf{T}^{-1^T} \mathbf{K}\, \mathbf{T}^{-1}; \quad \mathbf{F}^c = \mathbf{T}^T \mathbf{F}^{*c} \tag{29}$$

The second relation follows from the identities $\Delta U = \mathbf{q}^T\mathbf{F} = \mathbf{q}^{*T}\mathbf{F}^* = \mathbf{q}^T\mathbf{T}^T\mathbf{F}^*$, valid for any $\mathbf{q}$, and the first one follows from the identities $\mathbf{F} = \mathbf{K}\,\mathbf{q} = \mathbf{T}^T\mathbf{F}^* = \mathbf{T}^T(\mathbf{K}^*\mathbf{q}^*) = \mathbf{T}^T\mathbf{K}^*\,\mathbf{T}\,\mathbf{q}$, also valid for any $\mathbf{q}$.

Matrices $\mathbf{K}^*$ of the individual elements in global coordinates are finally assembled into the structural stiffness matrix, $\bar{\mathbf{K}}$, by the standard technique (41). The incremental equations of equilibrium of the structure read $\bar{\mathbf{K}}\,\bar{\mathbf{q}} = \bar{\mathbf{F}}$, in which q assembled column matrix of all generalized displacement increments of the structure; and $\bar{\mathbf{F}}$ = the associated column matrix of given increments of applied generalized forces.

Incremental Loading Procedure in Three Dimensions

For spatial large deflection analysis the same methods as for planar problems (1,19,24,29,37,41) can be applied. As is well known, two different methods of incremental analysis exist. In the first method the incremental properties of the material and the elements are all referred to the natural unstressed state [Lagrangian coordinate approach (15)] while in the second method they are referred to the current stressed state [Eulerian coordinate approach (15)] or, approximately, to the stressed state at the beginning of the current small time step, as is done herein for the purpose of numerical analysis. The first method is suitable, as a rule, when strains are large. But in the case that only displacements and rotations are large while material strains always remain small, as is assumed in this study and holds for nearly all practical thin-walled structures, the second method may be more expedient. In contrast with the first method (29,41), it has the advantage that the incremental stiffnesses depend only upon the current stresses (or, approximately, upon the initial stresses σ^0 of the current small increment, as indicated by Eq. 15) and are independent of the current displacements. This saves deriving several more types of matrices, 14 × 14 in size, which more than outweighs a disadvantage consisting in the fact that the second method requires the local coordinate systems of the elements to be up-dated

at each small load increment. Therefore, the second method has been adopted in the present study.

The loading vector, $\mathbf{f}$, is gradually incremented in small increments $\Delta\mathbf{f}_{(r)} = \mathbf{f}_{(r+1)} - \mathbf{f}_{(r)}$ ($r = 1, 2, \ldots$). The state of the structure at the beginning of the rth increment is characterized by global coordinates $X_{j(r)}, Y_{j(r)}, Z_{j(r)}$ of all joints $j = 1, 2, \ldots N_1$, by unit vectors $\mathbf{b}_{n(r)}$ giving the direction of the y-axis of the cross section of the nth element ($n = 1, 2, \ldots N_2$), and by the initial internal forces $P_{(r)}, M_{x(r)}, M_{y(r)}, \bar{B}_{(r)}$ in each element (Fig. 5). The computation of the changes due to the rth increment may be arranged in the following steps:

1. Using $P^0 = P_{(r)}$, $M_x^0 = M_{x(r)}$, $M_y^0 = M_{y(r)}$, $\bar{B}^0 = \bar{B}_{(r)}$, stiffness matrices $\mathbf{K}_n$ given by Eqs. 15 and 16 are computed for all elements ($n = 1, \ldots N_2$).
2. Unit axial vector $\mathbf{c}_{n(r)}$ of each element is determined from joint coordinates $X_{j(r)}, Y_{j(r)}, Z_{j(r)}$, and using vector $\mathbf{b}_{n(r)}$ and $\mathbf{a}_{n(r)} = \mathbf{c}_{n(r)} \times \mathbf{b}_{n(r)}$, rotation matrix $\mathbf{R}_{n(r)}$, Eq. 24, is set up for each element. The length of element may be determined from $X_{j(r)}, Y_{j(r)}, Z_{j(r)}$, but approximately may usually be taken the same as in the natural state.
3. Stiffness matrices $\mathbf{K}^*$ in global coordinates are computed from Eq. 29 and are assembled into the structural stiffness matrix, taking boundary conditions into account. Displacement increments $q^*_{(r)}$ due to load increment $\Delta f_{(r)}$ are then solved from a system of linear equations and the coordinates $X_{j(r+1)}, Y_{j(r+1)}, Z_{j(r+1)}$ of joints at the end of increment are evaluated.
4. Internal force increments at the ends of elements are computed as $\mathbf{F}^* = \mathbf{K}^*\, q^*_{(r)}$ for all elements and are transformed into local coordinates according to Eq. 29. Then the average increments of P, M_x, M_y, and B within the elements, and the final average values of $P_{(r+1)}, M_{x(r+1)}, M_{y(r+1)}$ within the element, are determined for all elements (as averages between the values at ends of elements).
5. Unit vector $\mathbf{b}_{n(r+1)}$ of the y-axis of each element at the end of increment may be determined from the average incremental rotation $\theta_n = (\theta_i + \theta_j)/2$ within the element about its axis. This rotation transforms vector $\mathbf{b}_{n(r)}$ into the vector

$$\mathbf{b}'_n = \mathbf{b}_{n(r)} + (\mathbf{c}_{n(r)} \times \mathbf{b}_{n(r)})\,\theta_n \tag{30}$$

which, however, is usually not exactly perpendicular to the z-axis unit vector $\mathbf{c}_{n(r+1)}$ determined from $X_{j(r+1)}, \ldots Z_{j(r+1)}$. Nevertheless, vector $\mathbf{b}'_n$ with $\mathbf{c}_{n(r+1)}$ determines plane (yz) at the end of increment and vector $\mathbf{b}_{n(r+1)}$ in this plane may thus be ascertained as the vector which is normal to $\mathbf{c}_{n(r+1)}$. Thus

$$\mathbf{b}_{n(r+1)} = (\mathbf{c}_{n(r+1)} \times \mathbf{b}'_{n(r+1)}) \times \mathbf{c}_{n(r+1)} \tag{31}$$

Note that rotations ξ' and $-\eta'$, if viewed as infinitesimally small, have no effect on orientation of plane yz.

6. Due to the numerical error arising from the finite size of the increments, there is always a certain small imbalance of the total forces (determined directly from total displacements) acting at each joint at the end of increment. To remove this error, the imbalance force must be subtracted from the given load increments in the subsequent iteration of this step.
7. In the foregoing procedure all element properties are based on the state at the beginning of the rth increment, and so the computed increments are

accurate only to the first order in $\Delta \mathbf{f}$, similarly as in the Euler method for ordinary differential equations. To reduce the error to the second order, a procedure similar to the second-order Runge-Kutta method may be used, i.e., steps 1 to 6 may be iterated basing all element properties on the state in the middle of the increment as determined from the previous analysis of the rth increment. Thus, denoting the averages between the initial and the final value in the rth step by subscript $(r + 1/2)$, e.g., $\bar{B}^0_{(r+1/2)} = (\bar{B}_{(r)} + \bar{B}_{(r+1)})/2$, the values $P^0 = P_{(r+1/2)}, \ldots, \bar{B}^0 = \bar{B}_{(r+1/2)}$ are used in step 1; in step 2, $\mathbf{c}_{n_{(r+1/2)}}$ and $\mathbf{R}_{n_{(r+1/2)}}$ are determined from $X_{j_{(r+1/2)}}, \ldots$ and $\mathbf{b}_{n_{(r+1/2)}}$; in step 5, Eq. 30 is modified as

$$\mathbf{b}'_n = \mathbf{b}_{n_{(r)}} + (\mathbf{c}_{n_{(r+1/2)}} \times \mathbf{b}_{n_{(r+1/2)}})\,\theta_n \quad \ldots\ldots\ldots\ldots\ldots\ldots\ldots\ldots\ldots\ldots \quad (32)$$

while Eq. 31 remains unchanged. Due to numerical errors vector $\mathbf{b}_{n_{(r+1/2)}}$ is

TABLE 1.—Numerical Results for Bifurcation-Type Lateral Buckling of Straight Beams

Number of elements (1)	Slenderness L/d (2)	Exact $M^0_{x_{cr}}$ (3)	$M^0_{x_{cr}}$ by finite elements (4)	Error, as a percentage (5)
4	10	627.40	627.89	0.08
8	38	101.4082	101.4106	0.002
16	38	101.4082	101.4089	0.0007
32	38	101.4082	101.4087	0.0005

Note: Moments are given in kip-in. (113 N-m).

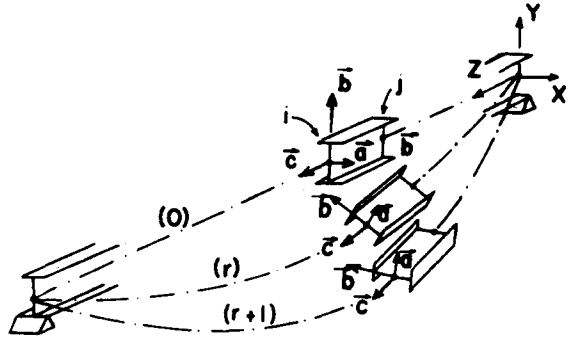

FIG. 5.—Straight-Element Approximations at Various Stages of Large-Deflection Lateral Buckling of I-beam (Numerical Example in Fig. 7)

not exactly of unit length and must therefore be normalized before evaluating Eq. 32.

8. Iterations of steps 1 to 6 as outlined in item 7 are carried out until the difference between the results of two consecutive iterations becomes negligibly small. Then the analysis proceeds to the $(r + 1)$st increment. Usually it is not advantageous to use more than about three iterations since further iterations improve accuracy less than a reduction in the load increment.

TABLE 2.—Numerical Results for Bifurcation

Case (1)	γ, in degrees (2)	Slenderness L/d (3)	EI_ω (4)	$M^0_{x_{cr}}$ for $R \to \infty$ (5)	Exact $M^0_{x_{cr}}$ (6)
a	30	12	$4C_1$	±3,995.2	4,734.6 −3,353.2
b	15	24	C_1	±627.4	748.6 −524.1
c	15	12	$4C_1$	±3,995.2	4,387.1 −3,696.4
d	7.5	12	$4C_1$	±3,995.2	4,165.6 −3,823.3
e	7.5	12	C_1	±2,128.5	2,256.3 −2,000.8

Note = Moments are given in kip-in. (113 N-m).

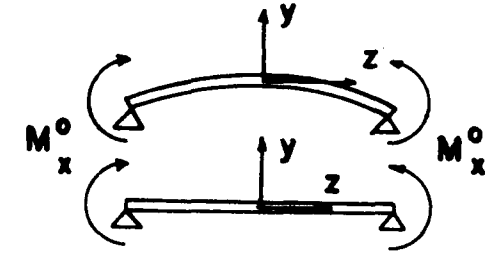

FIG. 6.—Simply Supported Beam or Circular Arch Under Uniform Initial Bending Moment

The foregoing procedure is applicable only on the increasing branch or on the decreasing branch of the load-displacement curve. At the limit point, at which the structural stiffness matrix becomes singular, it is possible to use various well-known techniques described, e.g., in Ref. 16.

The method presented in this study can be also applied to problems with inelastic strains (due to temperature, plastic yield, or creep), if the inelastic stresses are converted to applied loads.

Results of Numerical Studies

The accuracy of the proposed method of analysis has been examined by comparisons with exact analytical solutions. Such solutions exist only for bifurcation-type buckling problems and only for a few simple structural shapes and loadings.

Bifurcation-Type Bending-Torsional Buckling and Lateral Buckling of Straight Columns and Beams.—First the case of bending-torsional buckling of a straight pin-ended column under uniform axial force P^0 has been considered. The cross section properties were $EI_\omega = 1{,}024 \times 10^6$ kips-in^4 (1,896 kN-m^4), $GI_s = 60{,}000$ kips-in^2 (172,190 N-m^2), $EI_y = 2{,}580{,}000$ kips-in^2 (7,404 kN-m^2), x_0

Type Lateral Buckling of Circular Arches

$M^0_{x_{cr}}$ by finite elements (7)	ϵ_c, as a percentage (Eq. 35) (8)	Error, as a percentage (9)	Error/ϵ_c (10)
5,354.8	18.5	13.1	0.71
−3,068.2	−16.0	8.3	0.52
879.9	19.3	17.5	0.908
−454.7	−16.4	−13.2	0.805
4,467.3	9.81	1.83	0.187
−3,616.9	−7.48	−2.15	0.290
4,215.7	4.34	0.90	0.208
−3,793.2	−4.34	−0.68	0.157
2,352.3	6.1	4.2	0.689
−1,929.8	−6.1	−3.1	0.509

$= y_0 = 0$. Dividing the column of length 640 in. into eight elements, the computed bending-torsional buckling load differed from the exact value given by the formula in Ref. 38 only by 0.02% (upper bound result). For the two elements and a length of 160 in. (4,064 m) the error was 0.62%.

Then the cases of lateral buckling of beams were investigated. Simple exact formulas exist only when the beam is simply supported and M^0_x is constant along the beam, i.e., the beam is loaded by couples at its ends. The cross-sectional properties were the same as before. The error of the buckling load, P^0, with regard to the exact solution according to the formula given in Ref. 38 is tabulated in Table 1 for different numbers of elements. (L/d = span to beam depth ratio.) Obviously, excellent accuracy is easily attainable in the case of straight beams.

The eigenvalue problems arising in the analysis were solved by standard library subroutines. But when the size of the matrix was too large, the dependence of a certain suitably chosen stiffness parameter on the initial load was determined instead and its zero was found by the regula falsi method.

Bifurcation-Type Lateral Buckling of Arches.—Some simplified practical problems for lateral stability of arches have been solved numerically (30,36) for the case of simple torsion. Among thin-walled curved beam problems, a simple analytical solution exists only for a circular two-hinge arch, curved in plane yz and subjected to uniform initial moment M^0_x introduced at the ends which are free to rotate in plane yz but prevented to rotate in other planes (Fig. 6) (40,20). According to Chapter XII in Ref. 40, the smallest positive or negative critical moment is

$$M^0_{x_{cr}} = \alpha \pm \sqrt{\alpha^2 + \beta^2} \quad \ldots\ldots\ldots\ldots\ldots\ldots\ldots\ldots\ldots\ldots \quad (33)$$

in which the plus sign is for bending in the sense of initial curvature; the minus sign is for bending against it; and

$$\alpha = \frac{1}{2R}\left(EI_y + C + \frac{\pi^2}{L^2}C_1\right),$$

$$\beta = \left(\frac{\pi^2}{L^2} - \frac{1}{R^2}\right)EI_y C\left(1 + \pi^2 L^2 \frac{C}{C_1}\right) \quad \ldots\ldots\ldots\ldots\ldots\ldots\ldots\ldots \quad (34)$$

L = length of the arc between supports.

The cross section properties, GI_s and EI_y, considered in the practical examples, were again GI_s = 60,000 kips-in^2 (172,190 N-m^2), EI_y = 2,580,000 kips-in^2 (7,404 kN-m^2), $x_0 = y_0 = 0$, while two values of EI_ω were used as shown in Table 2 with $C_1 = 1{,}024 \times 10^6$ kips-in^4 (1,895,900 N-m^4). It has been found that with increasing numbers of elements the numerical results for the critical M^0_x converge quite rapidly (approximately as in Table 1), but frequently to a value which is substantially different from the exact solution. Some typical values of $M^0_{x_{cr}}$ to which the finite element analysis converged (values for 16 elements) are summarized in Table 2, for various lengths L of the beam (measured along the arc), central angles γ of the arc, and warping rigidities EI_ω.

In evaluating the numerical error, comparisons of the change in critical moment due to curvature of the beam were made. This change was characterized by the parameter

$$\epsilon_c = \frac{M^0_{x_{cr}} - M^0_{x_\infty}}{M^0_{x_\infty}} \quad \ldots\ldots\ldots\ldots\ldots\ldots\ldots\ldots\ldots\ldots\ldots\ldots \quad (35)$$

in which $M^0_{x_\infty}$ = exact critical bending moment for straight beam ($R \to \infty$) of the same cross section properties and length; and $M^0_{x_{cr}}$ = exact critical bending moment of the given curved beam. The numerical analysis may be considered to be a useful tool when the ratio of the numerical error to change ϵ_c due to curvature, as defined by Eq. 35, is small; i.e., less than about 1/3.

In general, it is seen from Table 2 that the numerical error is unacceptably large when: (1) The curvature is large; (2) the arch is slender, i.e., the length-to-depth ratio is large; and (3) the warping rigidity is small. In other cases (cases c and d in Table 2), the analysis proposed herein gives acceptable results. Below the buckling range the limitations are less stringent.

The fact that the numerical solution of buckling loads is poor for large curvatures and for slender arches is not surprising. Similar conclusions have recently been reached in the studies of finite elements for thin shells and for plane deformations of slender arches (3,4,5,13,25,35,37). From these studies it became clear that, in order to obtain a generally applicable planar finite element, a curved element will have to be developed. This need is probably due to the fact that only curved elements can guarantee full continuity of finite element subdivision (while for straight elements the end cross sections forming an angle overlap on one side of beam axis and leave a gap on the other side). For convergence to a correct value the shape functions must satisfy exactly the conditions that: (1) no self-straining occurs at rigid body rotations; and (2) all states of constant generalized strains are available. Satisfying these conditions with a curved element exactly is not easy.

Nevertheless, for many practical problems the present formulation appears to be satisfactory. While arches rarely have deep members and small enough curvatures, beams and frames do. They usually cannot develop very large curvature prior to failure of the material. In such cases the present large deflection analysis is applicable.

Large Deflection Lateral Buckling.—The foregoing method was applied to analyze post-critical lateral buckling of a simply supported I-beam under uniform vertical load (Figs. 5 and 7). The ends of beam were rotating freely in planes YZ and XZ, and translating freely in the Z direction, all other motions being prevented. The properties of the beam were: span L = 640 in., EI_y = 2,580,000 kips-in^2 (7,404 kN-m^2), GI_s = 60,000 kips-in^2 (172,190 N-m^2), EI_ω = 1,024 × 10^6 kips-in^4 (1,896 kN-m^4), EI_x = 234 × 10^6 kips-in^2 (672 × 10^6 N-m^2), $x_0 = y_0 = 0$, depth d = 40 in. (1.02 m). First, the critical load was found by computing the inverse rotation, θ_1, due to a fixed lateral loading moment applied on a beam under various initial vertical loads; plotting these values

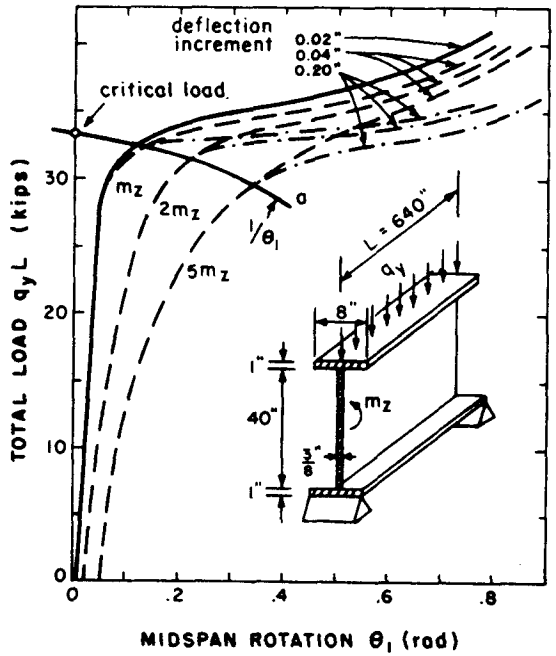

FIG. 7.—Computed Load-Rotation Curves for Large-Deflection Lateral Buckling (Results for Three Different Vertical Displacement Increments, and for Three Different Fixed Lateral Disturbing Distributed Moments m_z = 0.25 kips, $m_z/2$, $m_z/5$; 1 kip = 4,448 N)

gives curve a in Fig. 7 and the critical load is obtained as its intersection with the vertical axis by the regula falsi method.

For large-deflection analysis, the beam was considered to be disturbed by a small constant distributed applied moment m_z about global axis Z, initially coinciding with beam axis. The plot of lateral rotations versus vertical load is given in Fig. 7 for three values of the disturbing load. The increments of vertical distributed load were adjusted as to give constant increments of midspan deflection, for which three values were used. The results obviously converge with diminishing load increment.

One interesting observation from Fig. 7 is the fact that after exceeding the

critical load the beam stiffens, in a manner similar to columns or plates. The stiffening occurs at a relatively large deflection, so that the post-critical reserve of this beam is not usable.

Furthermore, large-deflection buckling of beams with asymmetric angle cross sections (Fig. 8) was computed and compared with the experimental results of Engel and Goodier (14), which have not yet been fitted by any theory, to the writers' knowledge. The comparison is excellent, which validates the present method of analysis.

Large Twist of Initially Bent Beams.—Fig. 9 shows a comparison for channel

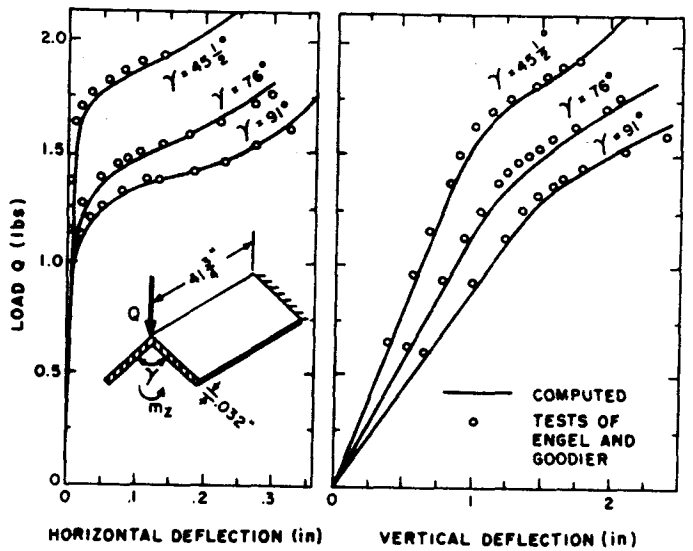

FIG. 8.—Computed Large-Deflection Lateral Buckling of Cantilever, Compared with Experiment of Engel and Goodier (14) (for Three Different Angles of Legs; Aluminum, E = 10 × 10^6 psi (6.89 × 10^4 N/mm^2);

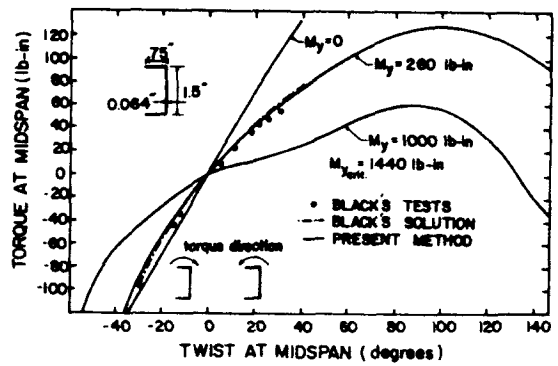

FIG. 9.—Comparison of Present Solution with Experimental Data and Analytical Solution of Black (10); Channel is Supported as in Fig. 7 and is Preloaded by Constant Uniform Load Causing Moment M_y (1 lb-in. = 113 N-mm)

sections with the tests and an approximate analytical solution of Black (10). [Since he has not reported M_y (Fig. 9), its value was deduced by fitting the data]. Integration through the limit point (peak of the curve in Fig. 9) was made possible by switching to prescribed displacement increments. A second, minimum limit point exists for twist angles exceeding the range in Fig. 9.

Summary and Conclusions

1. The general incremental stiffness matrix of straight thin-walled beam elements of generally asymmetric open cross section, subjected to initial axial force, initial bending moments, and initial bimoment, is presented.
2. The expression of incremental potential energy, from which this matrix was derived, was checked for giving the correct differential equations of the problem (40).
3. The transformation matrix relating the forces and displacements at the end cross sections of two elements meeting at an angle has been derived as the limiting case of a transfer matrix for a curved member. Noteworthy is the fact that warping parameter θ' and bimoment $\bar{B}$ transform with unity and are independent of all other generalized displacements and forces.
4. A relatively simple treatment of arbitrary asymmetric cross sections is made possible by referring some of the element displacements and forces to the centroid and others to the shear center. The transformation matrix to global coordinates then also includes transformation of all components to centroidal axes.
5. The incremental large-displacement analysis is formulated using the Eulerian coordinate approach with up-dating of the local coordinate systems at each load increment. The beams, curved either naturally or due to prior deformation, are imagined to be composed of straight elements meeting at angles.
6. Numerical comparisons with known exact solutions of some bifurcation-type stability problems have indicated that the accuracy of the proposed scheme is excellent for straight or almost straight beams. In the case that the beams are curved, either naturally or as a result of large deflections, the scheme is sufficiently accurate only if the curvature radius, the depth-to-span ratio, and the warping rigidity are sufficiently large. This fact is not due to the presence of warping and is not surprising since similar limitations have been found in the case of planar deformations of arches. A possible remedy is the development of appropriate curved elements.
7. Because of the aforementioned limitations, the method presented herein is usually applicable only to large deflections of straight beams, frames or slightly curved beams in which slenderness is not too high and excessive curvatures cannot arise prior to failure of the material. Below the buckling load range the slenderness and curvature limitations are less stringent.
8. The present method gives excellent agreement with known experimental data.
9. A numerical example showed that in lateral buckling of an I-beam there is a large postbuckling reserve which, however, is usable only if very large deflection is permitted.
10. A snap-through was found to occur in large twist of an initially bent channel beam. It is followed by a minimum limit point.
11. The method can also be used for classical small deflection problems of curved thin-wall beam structures without initial stress.

Acknowledgment

Computer funds provided by Northwestern University are gratefully acknowledged.

Appendix I.—Transfer Matrix of Beam Curved in Plane

The row of the transfer matrix which gives bimoment $B_{j'}$ at end j' in terms of state vector at end j (subscript $_j$) is characterized by the following equation that has been obtained by integrating Eq. 21:

$$B_{j'} = (0)\theta_j - \left(\frac{CL}{\kappa}\,\mathrm{sh}\kappa\right)\left(\theta' + \frac{\eta'}{R}\right)_j + \left\{ -\frac{R^2c^2L\,\mathrm{sh}\kappa}{\kappa(L^2 - c^2R^2)} + \frac{L^2R\sin\left(\frac{L}{R}\right)}{(L^2 - c^2R^2)} \right\} M_{z_j}$$

$$+ (\mathrm{ch}\kappa)B_j + (0)\eta_j + (0)\eta_j' + \left\{ \frac{RL^2\,\mathrm{ch}\kappa}{L^2 + \kappa^2R^2} - \frac{RL^2\cos\left(\frac{L}{R}\right)}{(L^2 + \kappa^2R^2)} \right\} M_{x_j}$$

$$+ \left\{ -\frac{RL^3\,\mathrm{sh}\kappa}{\kappa(L^2 - c^2R^2)} + \frac{R^2L^2\sin\left(\frac{L}{R}\right)}{(L^2 - c^2R^2)} \right\} V_{x_j} \quad \ldots\ldots\ldots\ldots\ldots (36)$$

This relation has been checked for giving at $R \to \infty$ the bimoment row of the well-known transfer matrix of a straight beam, i.e.:

$$B_j' = -(CL\kappa^{-1}\,\mathrm{sh}\kappa)\theta_j' + (L\kappa^{-1}\,\mathrm{sh}\,\kappa)M_{zj} + (\mathrm{ch}\,\kappa)B_j \quad \ldots\ldots\ldots\ldots (37)$$

The limiting case $R \to 0$ gives 1 in Eq. 22.

Appendix II.—References

1. Argyris, J. H., "Continua and Discontinua," *Proceedings*, Conference on Matrix Methods in Structural Mechanics, Air Force Institute of Technology, Wright Patterson A.F. Base, Ohio, 1965.
2. Argyris, J. H., and Radaj, D., "Steifigkeitsmatrizen dünnwandiger Stäbe und Stabsysteme," *Ingenieur-Archiv*, Vol. 40, 1971, pp. 198–210.
3. Ashwell, D. G., and Sabir, A. B., "Limitations of Certain Curved Finite Elements when Applied to Arches," *International Journal of Mechanical Sciences*, Vol. 13, 1971, pp. 133–139.
4. Ashwell, D. G., Sabir, A. B., and Roberts, T. M., "Further Studies in the Application of Curved Finite Elements to Circular Arches," *International Journal of Mechanical Sciences*, Vol. 13, 1971, pp. 507–517.

5. Austin, W. J. "In-Plane Bending and Buckling of Arches," *Journal of the Structural Division*, ASCE, Vol. 97, No. ST5, Proc. Paper 8130, May, 1971 (Disc., Vol. 98, No. ST7, July, 1972, p. 1670).
6. Barsoum, R., and Gallagher, R. H., "Finite Element Analysis of Torsional and Torsional-Flexural Stability Problems," *International Journal for Numerical Methods in Engineering*, Vol. 2, No. 3, 1970, pp. 335-352.
7. Bažant, Z. P. "Nonuniform Torsion of Thin-Walled Bars of Variable Cross Section," *International Association for Bridge and Structural Engineering, Publications*, Vol. 25, 1965, pp. 245-267 (see also *Inženýrské Stavby*, Prague, Czechoslovakia, Vol. 15, 1967, pp. 222-228).
8. Bažant, Z. P., "Pièces longues a voiles épais et calcul des poutres à section déformable," *Annales des Ponts et Chaussées*, No. III, 1969, pp. 115-169 (see also *Stavebnícky Časopis SAV*, Vol. 15, 1967, pp. 541-555).
9. Bažant, Z. P., "A Correlation Study of Formulations of Incremental Deformation and Stability of Continuous Bodies," *Transactions*, American Society of Mechanical Engineers, *Journal of Applied Mechanics*, Vol. 38, 1971, pp. 919-928.
10. Black, M., "Non-linear Behaviour of Thin-walled Unsymmetrical Beam-sections Subjected to Bending and Torsion," *Thin-walled Structures*, A. H. Chilver, ed., John Wiley and Sons, Inc., New York, N.Y., 1967, pp. 87-102.
11. Borisov, M. D., *Torsional Analysis of Beam and Frame Systems of Thin-Walled Composite Bars* (in Russian), Izd. Lit. po Stroit., Leningrad, U.S.S.R., 1970.
12. Bychkov, D. V., *Structural Mechanics of Thin-Walled Bar Structures* (in Russian), Gosstroyizdat, Moscow, 1962; see also *Analysis of Beam and Framed Systems of Thin-Walled Elements* (in Russian), Gosstroyizdat, Moscow, U.S.S.R., 1948.
13. Dawe, D. J. "Finite Deflection Analysis of Arches," *International Journal for Numeral Methods in Engineering*, Vol. 3, 1971, pp. 529-552.
14. Engel, H. L., and Goodier, J. N., "Measurements of Torsional Stiffness Changes and Instability due to Tension, Compression, and Bending," *Journal of Applied Mechanics, Transactions*, American Society of Mechanical Engineers, Vol. 20, 1953, pp. 553-560.
15. Fung, Y. C., *Foundations of Solid Mechanics*, Prentice Hall, Inc., Englewood Cliffs, N.J., 1965.
16. Gallagher, R. H., "Finite-element Method of Limit Point Calculation," presented at the October, 1972, ASCE Annual and National Environmental Engineering Meeting, held at Houston, Tex., (Preprint 1823).
17. Gorbunov, B. N., and Strel'bitskaya, A. I., *Theory of Frames of Thin-Walled Bars* (in Russian), Gostechizdat, Moscow, U.S.S.R., 1948.
18. Gregory, M., "Elastic Torsion of Members of Thin Open Cross-section," *Australian Journal of Applied Science*, Vol. 12, No. 2, June, 1961, p. 1974.
19. Hutchinson, J. W., and Koiter, W. T., "Post-Buckling Theory," *Applied Mechanics Reviews*, Vol. 23, 1970, pp. 1353-1366.
20. Kollar, L. "Torsional Buckling of Thin-Walled Curved Bars (Shell-Arches)," *Acta Technica*, Budapest, Hungary, Vol. 40, No. 3/4, 1962, pp. 337-353.
21. Kollbrunner, C. F., Hajdin, N., and Krajcinovic, D., "Matrix Analysis of Thin-Walled Structures," *Report No. 10, Institute for Engineering Research*, Verlag Leemann, Zürich, Switzerland, 1969.
22. Krahula, J. L., "Analysis of Bent and Twisted Bars using the Finite Element Method," *AIAA Journal*, Vol. 5, 1967, pp. 1194-1197.
23. Krajcinovic, D., "A Consistent Discrete Elements Technique for Thin-Walled Assemblages," *International Journal of Solids and Structures*, Vol. 5, 1969, pp. 639-662.
24. Marçal, P. V., "Effect of Initial Displacement on Problem of Large Deflection and Stability," *Technical Report ARPA E5 4*, Brown University, Providence, R.I., 1967.
25. Megard, G., "Planar and Curved Shell Elements," *Finite Element Methods in Stress Analysis*, I. Holand, and K. Bell, eds., Tapir-T.U., Trondheim, Norway, 1970, pp. 287-318.
26. Mei, C., "Coupled Vibrations of Thin-Walled Beams of Open Section using the Finite Element Method," *International Journal of Mechanical Sciences*, Vol. 12, 1970, pp. 883-891.
27. Mei, C., "Reply to Krajcinovic's Discussion," *International Journal of Mechanical Sciences*, Vol. 13, 1971, pp. 739-740.

28. Nowinski, J., "Theory of Thin-Walled Bars," *Applied Mechanics Reviews*, Vol. 12, No. 4, 1959; up-dated in *Applied Mechanics Surveys*, M. N. Abramson, et al., eds., Spartan Books, Washington, D.C., 1966, pp. 325-338.
29. Oden, T., *Finite Elements of Nonlinear Continua*, John Wiley and Sons, Inc., New York, N.Y., 1971.
30. Ostenfeld, A., "Seitensteifigkeit offener massiver Bogenbrücken," *Schweizerische Bauzeitung*, Vol. 77, No. 15 and 16, 1921.
31. Powell, G., and Klingner, R., "Elastic Lateral Buckling of Steel Beams," *Journal of the Structural Division*, ASCE, Vol. 96, No. ST9, Proc. Paper 7555, 1970, pp. 1919-1932.
32. Przemieniecki, J. S., *Theory of Matrix Structural Analysis*, McGraw-Hill Publishing Co., New York, N.Y., 1968.
33. Rajasekaran, S., "Finite Element Analysis of Thin-Walled Members of Open Section," thesis presented to the University of Alberta, at Edmonton, Canada, in 1971, in partial fulfillment of the requirements for the degree of Doctor of Philosophy.
34. Renton, J. D., "Buckling of Frames Composed of Thin-Walled Members," *Thin-Walled Structures*, A. H. Chilver, J. Wiley, ed., John Wiley and Sons, Inc., New York, N.Y., 1967, pp. 1-59 (see Eqs. 130-141).
35. Sabir, A. B., and Ashwell, D. G., "A Comparison of Curved Beam Finite Elements when used in Vibration Problems," *Journal of Sound and Vibration*, Vol. 18, 1971, pp. 555-563.
36. Stüssi, F., *Kippen und Querschwingungen von Bogenträgern, International Association for Bridge and Structural Engineering Publications*, Vol. 7, 1943, pp. 327-343.
37. Walker, A. C., "A Nonlinear Finite Element Analysis of Shallow Circular Arches," *International Journal of Solids and Structures*, Vol. 5, 1969, pp. 97-107.
38. Timoshenko, S. P., and Gere, J. M., *Theory of Elastic Stability*, 2nd ed., McGraw-Hill Publishing Co., New York, N.Y., 1961, pp. 212-277.
39. Urban, I. V., "Theory of the Analysis of Thin-Walled Bar Structures" (in Russian), *Izd. TZDI*, Moscow, U.S.S.R., 1955.
40. Vlasov, V. Z., *Thin-Walled Elastic Bars* (in Russian), 2nd ed., Fizmatgiz, Moscow, U.S.S.R., 1959 (also, English translation, Israel Program for Scientific Translations, Jerusalem, Israel, 1961; French translation, Eyrolles, Paris, France, 1962).
41. Zienkiewicz, O. C., *The Finite Element Method in Engineering Science*, McGraw-Hill Publishing Co., London, England, 1971.

Appendix III.—Basic Notations

The following symbols are used in this paper:

A, E, G = cross-sectional area, Young's and shear modulus;

$\mathbf{a}$, $\mathbf{b}$, $\mathbf{c}$ = unit vectors in Eq. 24 (Fig. 6);

B^0, M_x^0, M_y^0, P^0 = initial bimoment, bending moments and axial force (Eq. 2), (Fig. 1);

B, M_x, M_y, P = incremental values of B^0, M_x^0, M_y^0, P^0;

C, C_1 = parameters given by Eq. 17;

$\mathbf{F}$ = column matrix of generalized forces, Eq. 18;

GI_s = Saint-Venant's rigidity in simple torsion;

I_x, I_y = principal cross-sectional moments of inertia (about centroidal axes x and y);

I_ω = $\int_A \bar{\omega}^2 dA$ = principal sectorial moment of inertia (referred to shear center); EI_ω = warping rigidity of Timoshenko and Gere (38);

$\mathbf{K}$, $\mathbf{K}_1$, $\mathbf{K}_2$, $\mathbf{K}_3$, $\mathbf{K}_4$ = element stiffness matrix and geometrical stiffness matrices (Eq. 14);

l, L = length of element or length of beam along arc, respectively;

$\bar{M}_z, M_s$ = torque about shear center and St. Venant's torque;
$\mathbf{q}$ = column matrix of generalized displacements (Eq. 11);
$R, \mathbf{R}$ = radius of curvature and rotation matrix, Eq. 24;
r = parameter given by Eq. 9;
$\mathbf{S}, \mathbf{T}, \mathbf{T}'$ = state vector, transformation and transfer matrices, Eqs. 20, 27, 19;
$\mathbf{t}$ = matrix of transformation from shear center to centroid, given by Eq. 25;
u_x, u_y, u_z = lateral and longitudinal displacements, Eqs. 7, 1 (Fig. 1);
$\bar{V}_x, \bar{V}_y$ = shear forces in x and y directions;
$W, \bar{W}$ = parameters given by Eq. 9;
X, Y, Z = global cartesian coordinates (Fig. 6);
x, y, z = local cartesian coordinates of cross section or element (Fig. 1);
x_0, y_0 = coordinates of shear center;
β_x, β_y = parameters given by Eq. 10;
ΔU = incremental potential energy (Eq. 3);
κ = parameter given by Eq. 17;
$\bar{\xi}, \bar{\eta}, \zeta, \theta$ = displacements of cross section and its rotation about axis z (Fig. 1); and
$\omega, \bar{\omega}$ = sectorial coordinate (Eq. 1) with respect to centroid, and to shear center (ω differs only by constant from warping function ω_s of Timoshenko and Gere (38), their use of bars is different).

Subscripts.

i, j, k = joints;
n = elements; and
(r) = load increments.

Superscripts.

0 = initial internal forces;
$\tilde{}$ = quantities referred to shear center, without bar, referred to centroid; and
$( )'$ = $\partial/\partial z$.

10247 BUCKLING OF THIN-WALLED BEAMS AND FRAMES

KEY WORDS: Arches; **Beams (supports); Buckling;** Curved beams; Elastic properties; **Engineering mechanics;** Finite elements; **Frames; Matrix methods (structural);** Stability; **Thin-wall structures**

ABSTRACT: The potential energy expression and the (14 by 14) stiffness matrix of a straight thin-walled beam element of open asymmetric cross section, subjected to initial axial force, initial bending moments, and initial bimoment, are derived. The transformation matrix relating the forces and displacements (including bimoment and warping parameter) at the adjacent end cross section of two elements meeting at an angle is deduced as the limiting case of a transfer matrix of a curved beam. To cope with asymmetric cross sections, some element displacements and forces are referred to the shear center and others to the cross-sectional centroid, and the matrix for transformation from shear center to centroid is set up. The incremental large-displacement analysis is formulated using the Eulerian coordinate approach with updating of the local coordinate systems at each load increment. The deformed beams are imagined to be composed of straight elements. Results of lateral post-buckling analysis of various beams are presented.

REFERENCE: Bazant, Zdenek P., and El Nimeiri, Mahjoub, "Large-Deflection Spatial Buckling of Thin Walled Beams and Frames," *Journal of the Engineering Mechanics Division,* ASCE, Vol. 99, No. EM6, **Proc. Paper 10247,** December, 1973, pp. 1259-1281